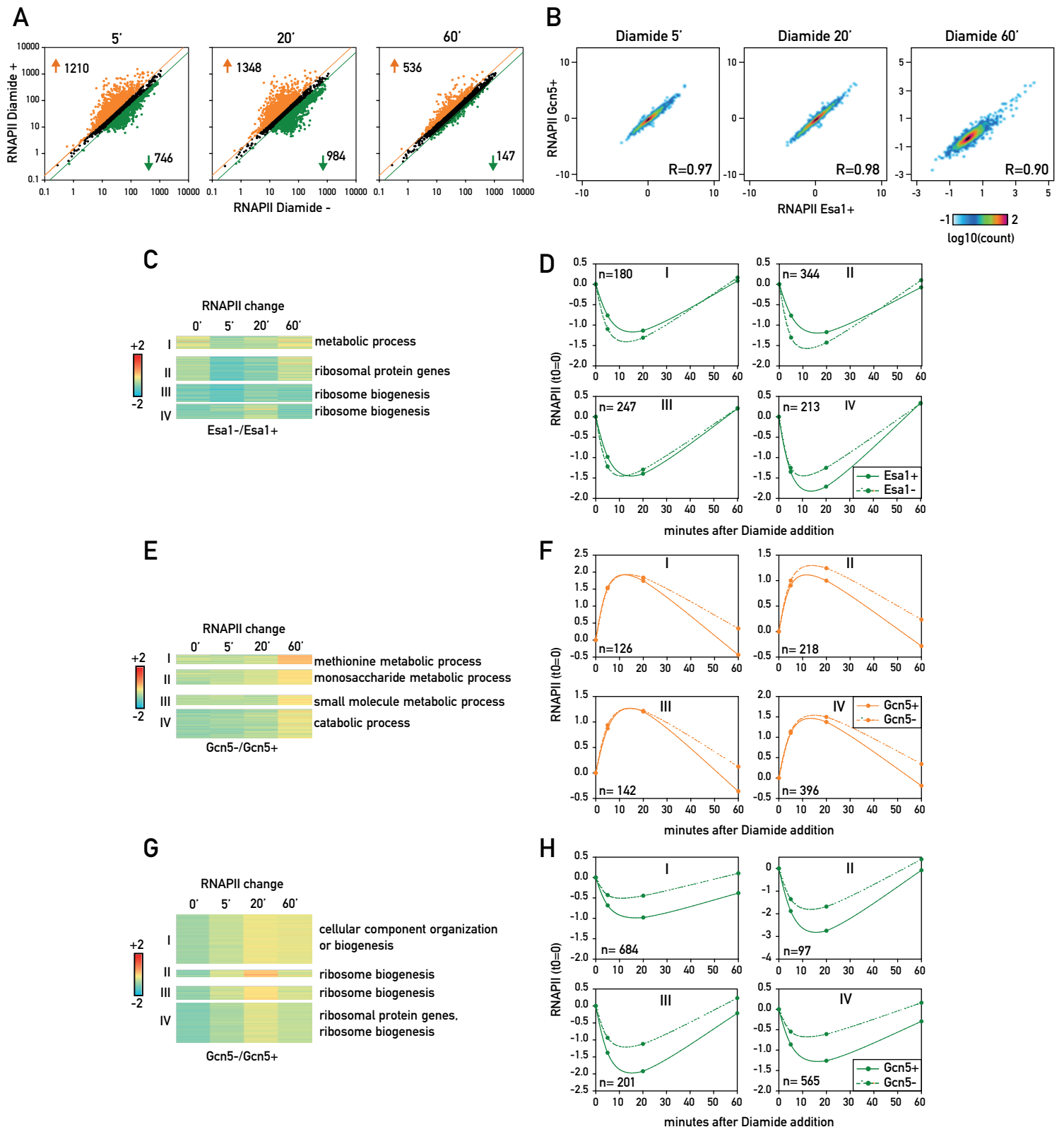
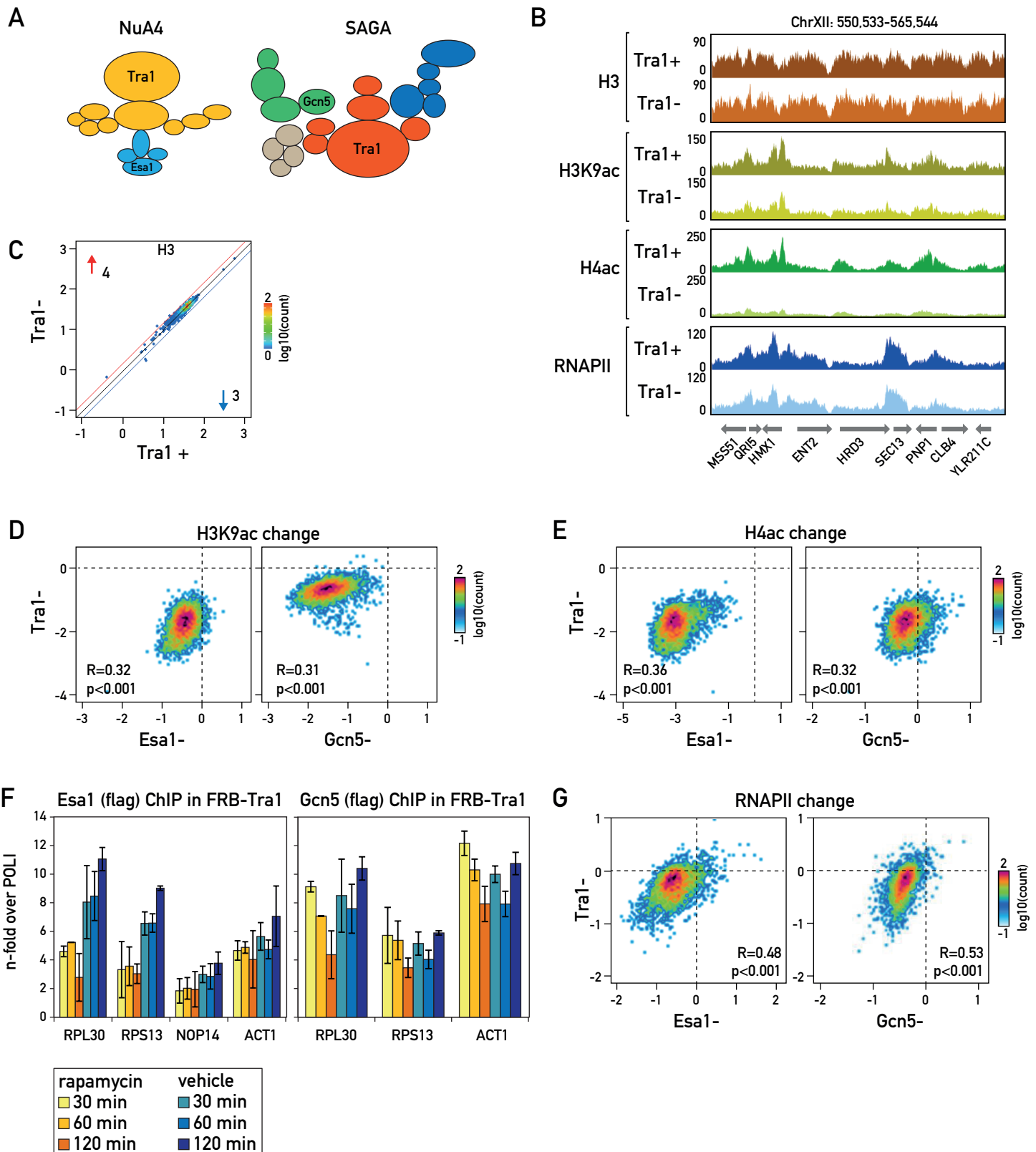


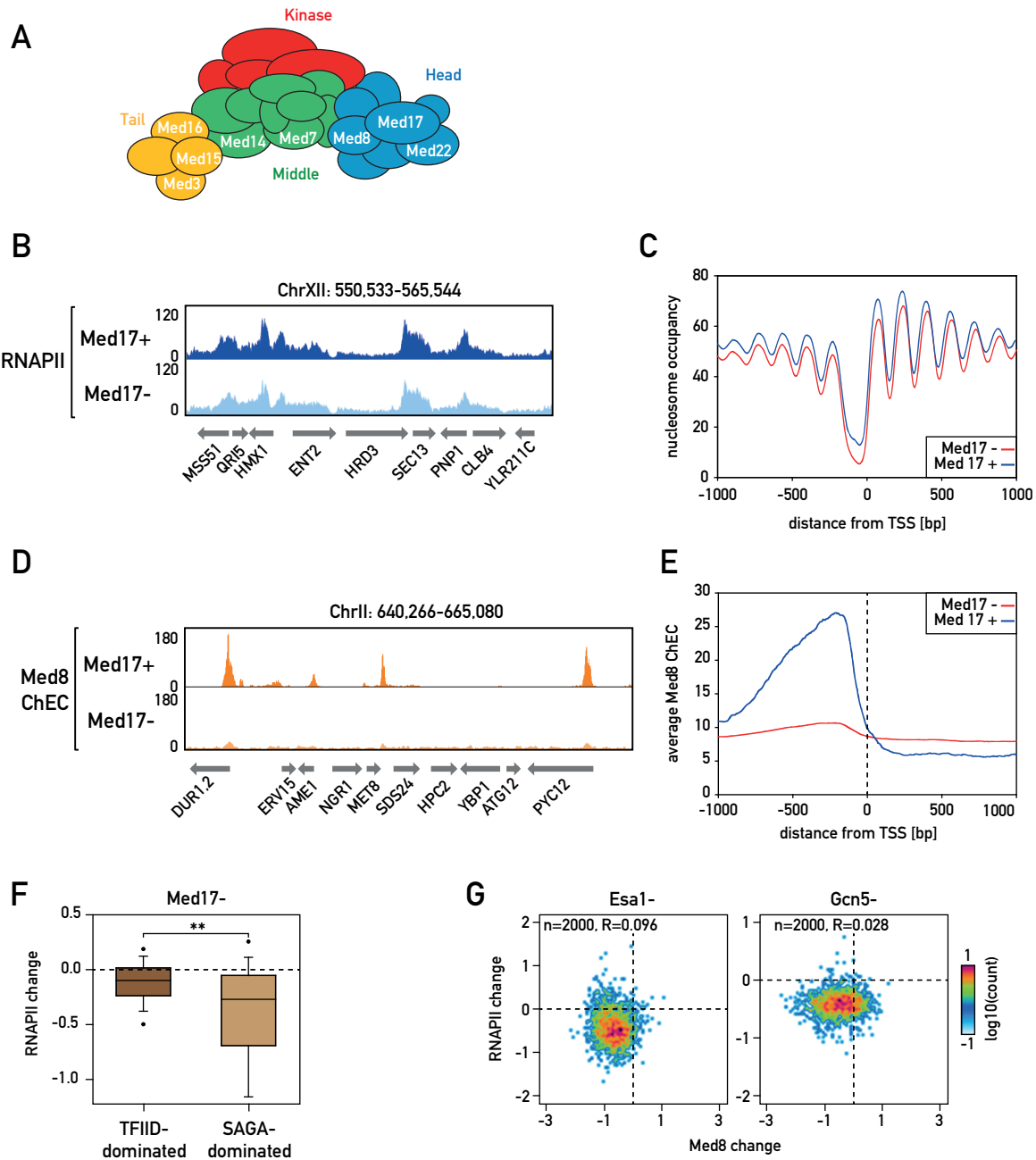
Supplemental Figure S1. (A) Ten-fold serial dilutions of the anchor-away strains used in this study on complete media minus or plus Rapamycin (1 µg/mL). Plates were imaged after 24 and 48 hours of growth at 30°C. (B) ChIP-qPCR of Epl1 (myc-tagged) in Esa1 nuclear-depleted (Esa1-) and non-depleted cells (Esa1+). UT: untagged control strain. (C) Genome Browser tracks showing the same region of Chromosome XII shown in Figure 1A for H3 and H3K9ac ChIP-Seq in Esa1 nuclear-depleted and non-depleted cells. (D) Scatterplots showing H3 (left) and H3K9ac (normalized to H3) (right) ChIP-Seq in Esa1 nuclear-depleted cells calculated and plotted as in Figure 1B. (E) Average nucleosome occupancy measured by MNase-Seq in Esa1 nuclear-depleted cells, calculated for the top 500 affected genes. (F) Scatterplot comparing the change in H4ac (normalized to H3, x-axis) and the change in RNAPII (y-axis) calculated as Log2 ratio between the signal in Esa1 nuclear-depleted cells and non-depleted cells (Esa1-/Esa1+) as in Figure 1C for Ribi genes (left) and RPGs (right). Pearson correlation coefficient and p-value are shown. (G) Genome Browser tracks as in (B) for H3 and H4ac in Gcn5 nuclear-depleted and non-depleted cells. (H) ChIP-qPCR of Ada2 (myc-tagged) in Gcn5 nuclear-depleted (Gcn5-) and non-depleted cells (Gcn5+). UT: untagged control strain. (I) Scatterplots showing H3 (left) and H4ac (normalized to H3, right) ChIP-Seq in Gcn5 nuclear-depleted cells calculated and plotted as in Figure 1B. (J) Average nucleosome occupancy measured by MNase-Seq in Gcn5 nuclear-depleted calculated on the top 500 affected genes. (K) Scatterplot comparing the change in H3K9ac (normalized to H3, x-axis) and the change in RNAPII (y-axis) for Gcn5 nuclear-depleted versus non-depleted cells calculated and plotted as in Figure 1C. (L) Box plots showing RNAPII change (calculated as in Figure 1E) in Esa1 and Gcn5 nuclear-depleted cells for 3991 genes categorized as TATA-depleted (TATA-, 3294 genes, light green) or TATA-containing (TATA+, 697 genes, dark green) according to Rhee and Pugh (2012). (M) Box plots showing RNAPII change in Gcn5 nuclear-depleted cells (calculated as in Figure 1E) for the top 525 affected genes (fold change > 1.5) categorized in TFIIID-dominated (396 genes) and SAGA-dominated (95 genes) according to (Huisinga and Pugh 2004).



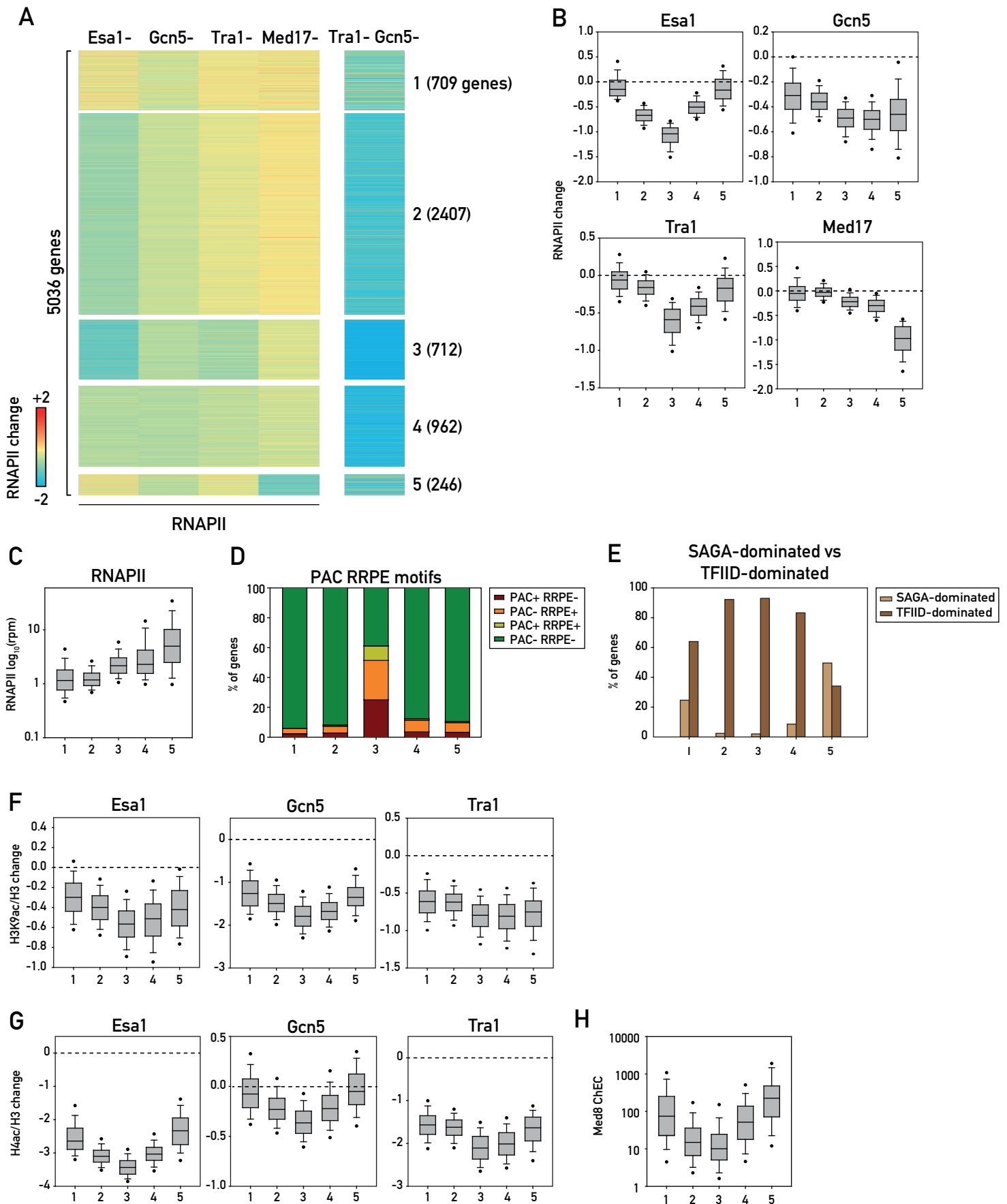
Supplemental Figure S2. (A) Scatterplots showing RNAPII ChIP-Seq in untreated cells (x-axis) versus diamide treated cells for 5 (left), 20 (middle) and 60 (right) minutes (y-axis). Each dot represents a gene. Orange and Green lines on the plots represent the threshold of 1.5-fold change. Genes have been classified in three groups according to their response to diamide: up-regulated in orange, down-regulated in green and not-affected (<1.5-fold change) in black. Data were derived from the *Esa1* anchor-away strain in the absence of rapamycin addition (no protein depletion). **(B)** Scatterplots showing correlation between RNAPII ChIP-Seq in diamide-treated *Esa1* anchor-away cells not treated with rapamycin (x-axis) versus *Gcn5* anchor-away cells not treated with rapamycin (left 5', middle 20', right 60' diamide). **(C)** Heatmap showing the RNAPII signal for the 984 diamide down-regulated genes for *Esa1* anchor-away experiment (as in Figure 2F) calculated and plotted as in Figure 2C. **(D)** Plots showing average RNAPII signal for the gene groups identified in (C) and plotted as in Figure 2B. **(E)** Heatmaps same as in (C) for diamide up-regulated genes for *Gcn5* anchor-away experiment (as in Figure 2G). **(F)** Plots same as in (D) for the gene groups identified in (E). **(G)** Heatmaps same as in (C) for diamide down-regulated genes for *Gcn5* anchor-away experiment (as in Figure 2H). **(H)** Plots same as in (D) for the gene groups identified in (G).



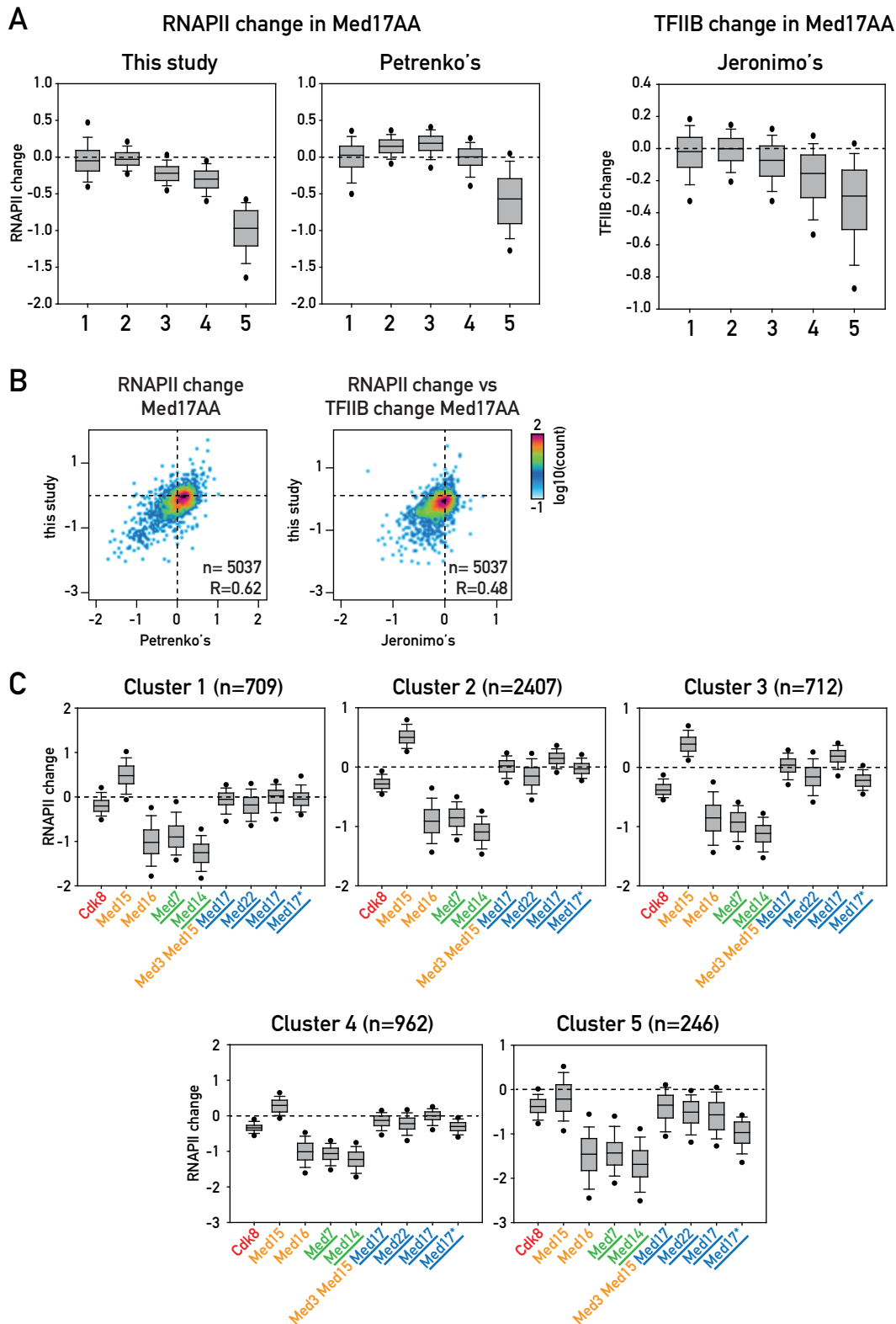
Supplemental Figure S3. (A) Schematic representation of the NuA4 and SAGA complexes as described in (Chittuluru et al. 2011; Lee et al. 2011). **(B)** Genome Browser tracks showing a region of Chromosome XII for H3, H3K9ac, H4ac and RNAPII ChIP-Seq in Tra1 nuclear-depleted and non-depleted cells. **(C)** Scatterplots showing H3 ChIP-Seq in Tra1 nuclear-depleted versus non-depleted cells calculated and plotted as in Figure 1B. **(D-E)** Scatterplots comparing the change in H3K9ac (D) and H4ac (E) occupancy normalized to H3 occupancy in Esa1 nuclear-depleted cells versus Tra1 nuclear-depleted cells (left) and Gcn5 nuclear-depleted cells versus Tra1 nuclear-depleted (right) calculated and plotted as in Figure 1C. **(F)** ChIP-qPCR of Gcn5 (flag-tagged) and Esa1 (flag-tagged) in Tra1-depleted (rapamycin) and non-depleted (vehicle) cells for the indicated time points. **(G)** Scatterplot comparing the change in RNAPII occupancy in Esa1 nuclear-depleted cells versus Tra1 nuclear-depleted (left) and Gcn5 nuclear-depleted cells versus Tra1 nuclear-depleted (right) cells, calculated and plotted as in Figure 1C.



Supplemental Figure S4. (A) Schematic representation of the Mediator complex. (B) Genome Browser tracks showing a region of Chromosome XII for RNAPII ChIP-Seq in Med17 nuclear-depleted and non-depleted cells. (C) Average nucleosome occupancy measured by MNase-Seq in Med17 nuclear-depleted and non-depleted cells calculated on the top 500 affected genes. (D) Genome Browser tracks showing a region of Chromosome II for Med8 ChEC in Med17 nuclear depleted and non-depleted cells. (E) Average Med8 occupancy measured by ChEC-Seq in Med17 nuclear depleted cells calculated in a window of 2kb centered on TSS for 5037 genes. (F) Box plots showing RNAPII change in Med17 nuclear depleted cells for 4682 genes categorized and plotted as in Figure 1E. (G) Scatterplots comparing the change in Med8 binding (x-axis) and RNAPII occupancy (y-axis) in *Esa1* nuclear depleted (left panel) and *Gcn5* nuclear depleted cells (right panel) for the 2000 UASs showing the strongest Med8 binding calculated and plotted as in Figure 1C.



Supplemental Figure S5. (A) Same heatmap as in Figure 5A with addition of a column showing RNAPII change in *Gcn5* and *Tra1* double depleted cells for the genes in the five clusters. **(B)** Box plots showing RNAPII change for each of the five clusters in *Esa1*, *Gcn5*, *Tra1* and *Med17* nuclear depleted cells. **(C)** Box plots showing RNAPII occupancy measured by ChIP-Seq for the genes in the five clusters. **(D)** Bar plots showing the percentage of genes classified according to the presence of PAC and RRPE motifs in their promoters for each of the five clusters. **(E)** Bar plots showing the percentage of genes defined as SAGA-dominated (light brown) and TFIID-dominated (dark brown) as reported in (Huisinga and Pugh 2004) for each of the five clusters. **(F-G)** Box plots showing H3K9ac (F) and H4ac (G) change for each of the five clusters in *Esa1*, *Gcn5* and *Tra1* nuclear depleted cells. **(H)** Box plots showing Med8 occupancy measured by ChEC for the genes in the five clusters.



Supplemental Figure S6. (A) Box plots showing RNAPII ChIP-Seq change in Med17 depleted cells versus non-depleted cells (calculated as Log_2 ratio Med17 depleted cells versus non-depleted cells) for data from this study (left panel) and from data from Petrenko et al. (2017) (middle panel) for the genes in the five gene clusters calculated and plotted as in Figure 1B. Right panel displays box plots showing TFIIB ChIP-chip signal change in Med17 depleted cells versus non-depleted cells calculated and plotted as for left and middle panels for data from Jeronimo et al. (2014). **(B)** Scatterplots showing RNAPII change in Med17 depleted cells versus non-depleted cells for data from this study and data from Petrenko et al. (2017) (left panel) and RNAPII change versus TFIIB change in Med17 depleted cells versus non-depleted for data from this study and data from Jeronimo et al. (2014). **(C)** Box plots showing RNAPII ChIP-Seq change calculated as in (A) in cells depleted for the Mediator subunits indicated for the five gene clusters. The different colors indicate different Mediator modules (red for Cdk8 module, yellow for tail module, green for middle module and blue for the head module). Med17* indicates data from this study, all the data for the other subunits are from Petrenko et al. (2017). Subunits essential for cell viability are underlined.

References

- Chittuluru JR, Chaban Y, Monnet-Saksouk J, Carrozza MJ, Sapountzi V, Selleck W, Huang J, Uteley RT, Cramet M, Allard S et al. 2011. Structure and nucleosome interaction of the yeast NuA4 and Piccolo-NuA4 histone acetyltransferase complexes. *Nat Struct Mol Biol* **18**: 1196-1203.
- Huisinga KL, Pugh BF. 2004. A genome-wide housekeeping role for TFIID and a highly regulated stress-related role for SAGA in *Saccharomyces cerevisiae*. *Mol Cell* **13**: 573-585.
- Jeronimo C, Robert F. 2014. Kin28 regulates the transient association of Mediator with core promoters. *Nat Struct Mol Biol* **21**: 449-455.
- Lee KK, Sardi ME, Swanson SK, Gilmore JM, Torok M, Grant PA, Florens L, Workman JL, Washburn MP. 2011. Combinatorial depletion analysis to assemble the network architecture of the SAGA and ADA chromatin remodeling complexes. *Mol Syst Biol* **7**: 503.
- Petrenko N, Jin Y, Wong KH, Struhl K. 2017. Evidence that Mediator is essential for Pol II transcription, but is not a required component of the preinitiation complex in vivo. *Elife* **6**.
- Rhee HS, Pugh BF. 2012. Genome-wide structure and organization of eukaryotic pre-initiation complexes. *Nature* **483**: 295-301.